NJC

Accepted Manuscript

Volume 40 | Number 1 | January 2016 | Pages 1–846

NJC

New Journal of Chemistry
www.rsc.org/njc

A journal for new directions in chemistry

ISSN 1144-0546

ROYAL SOCIETY
OF CHEMISTRY

PAPER
Jason B. Benedict et al
The role of atropisomers on the photo-reactivity and fatigue of
diarylethene-based metal–organic frameworks

cnrs

ROYAL SOCIETY
OF CHEMISTRY

rsc.li/njc

Journal Name

ARTICLE

Hydrogenation of hydrophobic substrates catalyzed by gold nanoparticles embedded in Tetronics/cyclodextrin-based hydrogels

M. Chevry[a], S. Menuel[a], B. Léger[a,*], S. Noël[a], E. Monflier[a] and F. Hapiot[a,*]

Hydrogenation of alkenes, alkynes and aldehydes was investigated under biphasic conditions using Au nanoparticles (AuNP) embedded into combinations of α-cyclodextrin (α-CD) and poloxamines (Tetronics®90R4). Thermo-responsive AuNP-containing α-CD/Tetronics®90R4 hydrogels are formed under well-defined conditions of concentration. AuNP displayed an average size of ca. 7 nm and a narrow distribution, as determined by TEM. The AuNP/α-CD/Tetronics®90R4 system proved to be stable over time. Upon heating above the gel-to-sol transition temperature, the studied catalytic system allowed hydrogenation of a wide range of substrates such as alkenes, alkynes and aldehydes under biphasic conditions. Upon repeated heating/cooling cycles, the Au NP/α-CD/Tetronics®90R4 catalytic system could be recycled several times without significant decline in catalytic activity.

Introduction

Since the emergence of synthetic catalysts during the 19th century, the search for effective catalytic systems have been receiving great attention. Although significant progresses have been made in terms of catalytic activity and selectivities, efforts should still be made to both recover and recycle the catalyst once the reaction is complete. During the past twenty years, we have been developing catalytic systems capable of ensuring high catalytic performance and reusability of organometallic or metallic catalysts.[1-3] Most of our strategies rely on cyclodextrins (CDs) which are cyclic oligosaccharides consisting of glucopyranose units linked by α-D-1,4-glycosidic bonds (Fig. 1).[4] Among the latest developments, one of our idea is to benefit from the ability of α-CD (6 glucopyranose units) to form thermoresponsive hydrogels by inclusion of organic molecules or polymer chain within their hydrophobic cavity.[5] At room temperature, such hydrogels are in the gel phase wherein they can efficiently stabilize organometallic and nanoparticle catalysts. When they are heated beyond their gel-to-sol transition temperature, the catalyst-containing gel phase turn into a sol phase. Upon stirring of the resulting catalyst-containing sol phase and a liquid organic substrate, the latter is converted into the corresponding product. Once the reaction is complete, the system is cooled down below the gel-to-sol transition temperature. The hydrogel returns to the gel phase and the catalyst and the product are easily recovered separately in two different phases.
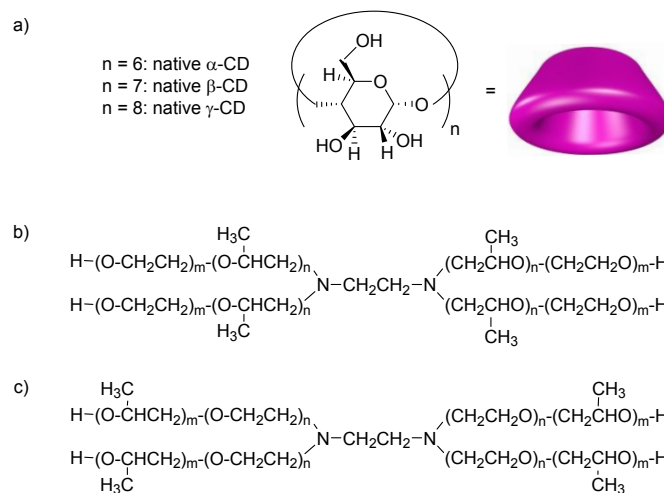

Fig. 1 Structure of a) cyclodextrins (CDs) and b) conventional sequential poloxamines and c) reverse-sequential poloxamines.

The concept has been developed for several applications. For example, Rh-catalysts embedded within α-CD/PEO (polyethylene oxide) hydrogels proved to be effective in the hydroformylation of very hydrophobic alkenes (>C12).[6,7] Ruthenium nanoparticles (RuNP) dispersed in a supramolecular CD-based hydrogel matrix showed great catalytic activity in hydrogenation of alkenes.[8] Interesting results were also obtained with α-CD and poloxamines (also known as Tetronics® macromolecules). The latter consist of block copolymers based on hydrophilic PEO and hydrophobic polypropylene oxide (PPO) attached on an ethylene diamine spacer.[9] Their X-shaped structure differs from the linear chains of poloxamers (Pluronics® macromolecules). Conventional sequential Tetronics® consist of PEO blocks at the outer sphere and PPO blocks attached to the diaminoethylene core, while reverse-sequential poloxamines

a. Univ. Artois, CNRS, Centrale Lille, ENSCL, Univ. Lille, UMR 8181, Unité de Catalyse et de Chimie du Solide (UCCS), F-62300 Lens, France.
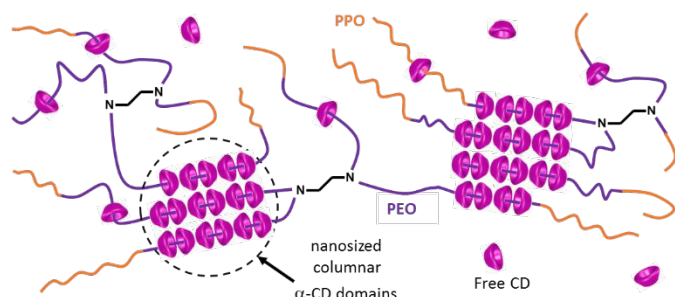
show PPO blocks at the periphery and PEO attached to the central diamino moiety (Fig. 1). α-CDs slide along the PPO/PEO copolymer blocks and selectively accommodate the PEO blocks. The threaded α-CDs form stacked nanocylinders that further aggregate into nanosized columnar α-CD domains through non-covalent interactions (Fig. 2).[10,11]

Fig. 2 Polypseudorotaxane aggregates of α-CD / reverse-sequential poloxamines (Tetronic®90R4).

Using Rh-catalyst embedded within α-CD/Tetronics® hydrogels, hydrophobic alkenes were efficiently converted into their corresponding aldehydes.[12] The catalytic performance remains unchanged upon recycling as the α-CD/Tetronics® hydrogel matrix prevents the oxidation of the phosphane (ligand stabilizing the Rh catalytic species).

In the light of the previous results, we have sought to extend the use of α-CD/Tetronics® hydrogels to nanoparticle catalysts, especially gold nanoparticles (AuNP). Although combination of AuNP, hydrogels and CDs has already been reported in the literature,[13-18] few has been devoted so far to the application of the resulting system in catalysis.[19] Reported herein is the AuNP-catalyzed hydrogenation of alkenes. Emphasis is especially on the reusability of the catalytic system.

Materials and methods

Reagents

Gold (III) chloride (99.9% - Au) was purchased from Strem Chemicals. Styrene, 1-heptyne, 1-octyne, 1-nonyne, 1-octene, 1-decene, 1-dodecene, *trans*-2-octene, α and β -pinenes were purchased from Acros. Cinnamaldehyde and benzaldehyde were purchased from Fischer. Tetronics®90R4, allylbenzene, phenylacetylene, methyl oleate, methyl linoleate and citronellal were purchased from Sigma Aldrich. α-CD was purchased from Wacker. All the chemicals and solvents were used as received without further purification.

Characterization techniques

A Brookfield Model LVDVII+Pro viscometer with the SC4-25 spindle at 20 rpm was used in this study. Viscosity was measured for temperatures ranging from 4 to 85 °C into a SC4-13RPY sample chamber with embedded RTD temperature probe. The temperature was controlled with a TC502 circulating bath refrigerated using a

programmable controller. The sample volume was slightly adapted to the volume of the sample chamber. The program parameters and results analysis were controlled with the Rheocalc@ PC Software. The UV-vis spectrophotometry analysis was carried out with a Perkin Elmer Lambda 19 UV-Vis spectrophotometer. 0.25 mL of the reaction mixture (with or without α-CD) are diluted in 2 mL of deionized water in order to get a transparent pink-purple solution. Transmission Electron Microscopy (TEM) was performed on a Tecnai microscope (200 kV). A drop of the colloidal suspension was deposited onto a carbon coated copper grid. Metal particle size distributions have been determined from the measurement of around 400 particles found in arbitrarily chosen area of the images using the program SCION Image.

Colloidal suspension synthesis

A Tetronics®90R4 solution (1250 mg in 2.5 mL of deionized water, 0.17 mmol) was stirred at 40 °C during 30 minutes at 1000 rpm. Then, 2.5 mL of an AuCl₃ solution ([Au] ranging from 0.1 to 2 mM) was added and the resulting solution was stirred at 40 °C during 1h at 1000 rpm. Finally, 725 mg (0.75 mmol) of α-CD were added and the mixture was stirred at 40 °C during 30 min at 1000 rpm. The flask was put in the fridge overnight to facilitate the sol-to-gel transition.

Catalytic experiment

All hydrogenation experiments have been performed using a Parker-Autoclave Engineers stainless steel autoclave containing the AuNP@α-CD/Tetronics®90R4 colloidal suspension in a glass vessel. The mixture was heated up to 50 °C with a thermostated oil bath in order to work beyond the gel-to-sol transition temperature. The substrate was added, the reactor was purged three times with nitrogen and hydrogen was fed to the system at constant pressure up to 40 bar. The reaction composition was determined after taking 0.25 mL of the reaction mixture which was diluted in 1 mL of water. The organic products were extracted with 0.5 mL of chloroform and analyzed by gas chromatography with a Varian 3900 gas chromatograph, equipped with a CP-Sil-5B (30 m × 0.25 mm x 0.25 μm) and a flame ionization detector, using decane or dodecane as external standard.

For the recycling experiments, after the first run, all the reaction compounds (styrene and ethylbenzene) were extracted several times with **chloroform** (5mL) until complete elimination of the organic products. Then, the organic phase was separated from the colloidal suspension after cooling down below the gel-to-sol transition temperature and the traces of **chloroform** were removed by purging the hydrogel phase with nitrogen during 10 minutes. Finally, after heating up to 50 °C, AuNP@α-CD/Tetronics®90R4 colloidal suspension was reloaded with styrene and dihydrogen and reused in the autoclave under the same experimental conditions (40 bar H₂, 50 °C).

Results and discussion

Synthesis of hydrogel-embedded AuNP

Given our previous results on the use of Tetronics® in hydroformylation,[12] the reverse-sequential Tetronic®90R4 (Mw 7200, 16 EO and 18 PO units per arm) was considered as poloxamine in the present study. Contrary to procedures described in the literature for which $HAuCl_4$ was used as Au precursor,[20] we used $AuCl_3$ whose fast reduction in an aqueous solution of Tetronics®90R4 (0.17 mmol in 5 mL water) led to AuNP at 40 °C. A small sacrificial quantity of Tetronics® acted as reductive agent thanks to terminal hydroxyl groups of Tetronics®[21] and imparted a pink color characteristic of the presence of AuNP to the solution (Supporting Information, Fig. S1). The AuNP embedded in the hydrogel matrix (AuNP@Tetronics®90R4) were characterized by UV spectrometry ([Au]=0.5 mM). UV spectra displayed in Fig. 3 confirmed the reduction of gold salts by the terminal hydroxyl groups of Tetronics® as a strong absorption band appeared at 532 nm due to the surface plasmon resonance of AuNP.[22] Interestingly, a red shift was observed from 532 to 547 nm after 90 min, which could be explained by an increase in the nanoparticle size.[23]
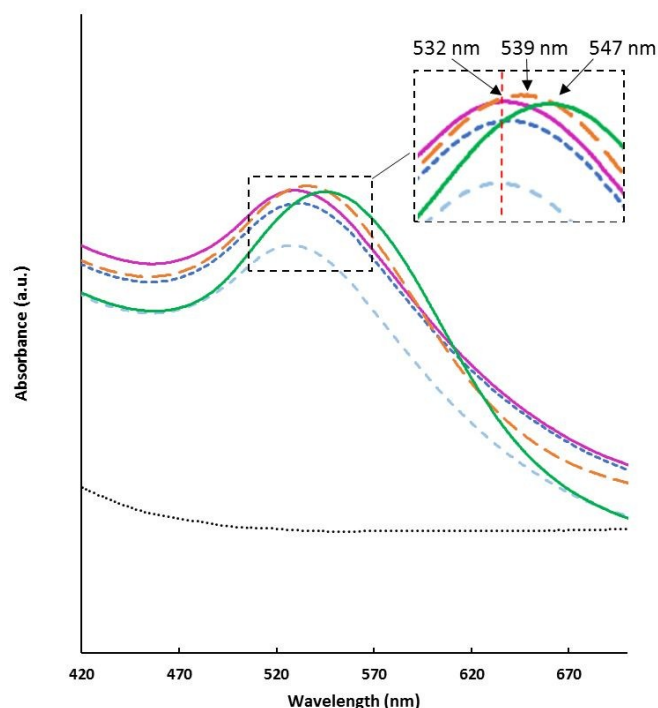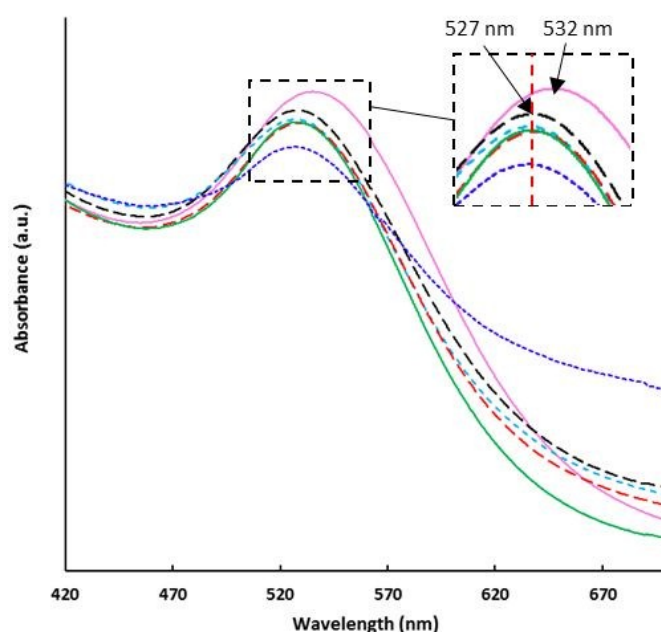

Fig. 3 Liquid UV spectra of hydrogel embedded AuNPs. [Au] = 0.5 mM, and Tetronics®90R4 (1250 mg) in water (5 mL) at 40°C at different reaction times, considering the start time t_0 as the instant where α-CD was added to the reaction medium. ··· t_0; —— $t_0 + 15$ min; --- $t_0 + 30$ min; —— $t_0 + 60$ min; —— $t_0 + 90$ min; —— $t_0 + 18$ h.

AuNP@Tetronics®90R4 were further characterized by transmission electronic microscopy (TEM). The bimodal distribution of AuNP observed after 30 min reaction time (two populations respectively centered at a mean diameter of 3.9 and 8.1 nm) suggested that the growth of AuNP was incomplete (Supporting Information, Fig. S2).

Conversely, small size and narrow Gaussian distribution characterized AuNP with a mean diameter of 7.7 nm after 60 min. Longer reaction time had deleterious effect on both the AuNP size and their distribution. Indeed, increase in the AuNP size and loss of the Gaussian shape of the size distribution were noticed after 90 min, indicative of the relative poor stability of the system over time in the absence of α-CD.

To prevent the formation of larger AuNP, another AuNP synthesis was carried out by addition of α-CD (0.75 mmol) in the Au/Tetronics® solution after 60 min. Upon heating at 40 °C, α-CD slided along the copolymer chain. Upon cooling down the system to room temperature, the sol phase turned into a AuNP-containing hydrogel (AuNP@α-CD/Tetronics®90R4). UV analysis revealed that addition of α-CD provoked a blue shift of λ_{max} from 532 to 527 nm (Fig. 4), indicative of a change in the environment around the AuNP.[22,24]

Fig. 4 Liquid UV spectra of hydrogel embedded AuNPs. [Au] = 0.5 mM, Tetronics®90R4 (1250 mg) and α–CD (750 mg) in water (5 mL) at 40°C at different reaction times, considering the start time t_0 as the instant where α-CD was added to the reaction medium. —— t_0; —— $t_0 + 1$ h; —— $t_0 + 3$ h; —— $t_0 + 5$ h; —— $t_0 + 18$ h; --- after 10 consecutive sol/gel transitions.

However, no further variation of λ_{max} was noticed for longer reaction time after addition of α-CD, suggesting that the α-CD/Tetronics® combination led to a better AuNP stabilization over time than Tetronics® used alone. The ability of the α-CD/Tetronics® matrix to protect efficiently the Au NPs from aggregation results from the additional effects of steric stabilization due to PEO/PPO polymer chains,[25-27] nitrogen atoms from ethylene diamine spacer[28] and the presence of α-CD.[29-34] Further evidence of the increased stability of AuNP@α-CD/Tetronics®90R4 regarding the system without α-CD was given by repeated heating/cooling cycles. We first determined the sol/gel transition temperature, which was established at 25 °C by viscosity measurements (Supporting Information, Fig. S3). While the viscosity of the gel was slightly influenced by the presence of AuNP, no variation of the viscosity was noticed in the sol phase.

ARTICLE

Secondly, upon heating and cooling down the system repeatedly, no modification of the AuNP shape or size was detected by TEM, indicative of the robustness of the AuNP@α-CD/Tetronics®90R4 system (Supporting Information, Fig. S4). Crystalline domains are shown on TEM image at a magnification of 490K with the presence of distinct lattice planes, which can be further analyzed using reduced Fast Fourier Transform (FFT)-derived diffraction patterns (Supporting Information, Fig. S5). The FFT-derived diffraction pattern indicates that the diffraction spot could be identified as Au nanocrystals with a face-centered-cubic (fcc) structure, based on the reflection from the (111) planes having a typical d-spacing of 0.23 nm.

Various concentrations of $AuCl_3$ ranging from 0.1 mM to 2 mM were also considered to assess the variation of the AuNP shape, size and distribution (Fig. 5). Transmission electron micrographs revealed that the spherical shape of AuNP was not altered upon increasing [Au]. The observation is in line with literature data that establish that the AuNP size is dependent upon the nature of the stabilizer (anionic, cationic…) or reducing agent concentration.[35,36] In fact, both α-CD and Tetronics®90R4 participate in the controlled growth of the AuNP through a "soft template" effect.[37-39] The presence of Tetronics®-constitutive nitrogens probably reinforce the stabilization of AuNP in the hydrogel matrix because of interactions between nitrogen atoms and the AuNP surface.[40-42] The average AuNP size was only slightly affected by variation in Au concentration, with mean diameter ranging from 7.4 to 7.7 nm. Conversely, the distribution was more influenced by the initial $AuCl_3$ concentration. From [Au] ranging from 0.5 to 1.5 mM, the distribution resembled a Gaussian curve while it was more polydisperse at [Au] = 2.0 mM.

AuNP-catalyzed hydrogenation of styrene

The catalytic performance of AuNP@α-CD/Tetronics®90R4 was assessed in hydrogenation of alkenes under 40 bar of H_2 at 50 °C (sol phase) for 30 min. Styrene was first chosen as a model substrate (Table 1). No trace of ethylcyclohexane could be detected once the reaction was complete. Ethylbenzene was exclusively formed, indicative of the high chemoselectivity of the reduction. Increasing the concentrations of $AuCl_3$ led to a regular decrease in conversion. We first thought that increasing the amount of $AuCl_3$ would lead to larger AuNP that would be responsible for the drop in conversion. However, as no significant variation of the AuNP size was noticed by TEM within the considered concentration range (Fig. 5), the reason of the drop in conversion probably lies in the increasing amount of chloride that limited the diffusion of the substrate at the aqueous/organic interface (salting-out effect).[43-45] Acidification of the medium by increasing amounts of chloride could also be a valid reason. Moreover, previous DFT studies clearly show that a strong interaction between chloride and Au(111) surface has been calculated[46,47] and could explain these catalytic results. Note that the viscosity of the α-CD/Tetronics®90R4 hydrogel could not be incriminated in the sol phase as it did not vary upon addition of AuNP, irrespective of the Au concentration (Supporting Information, Fig. S3).
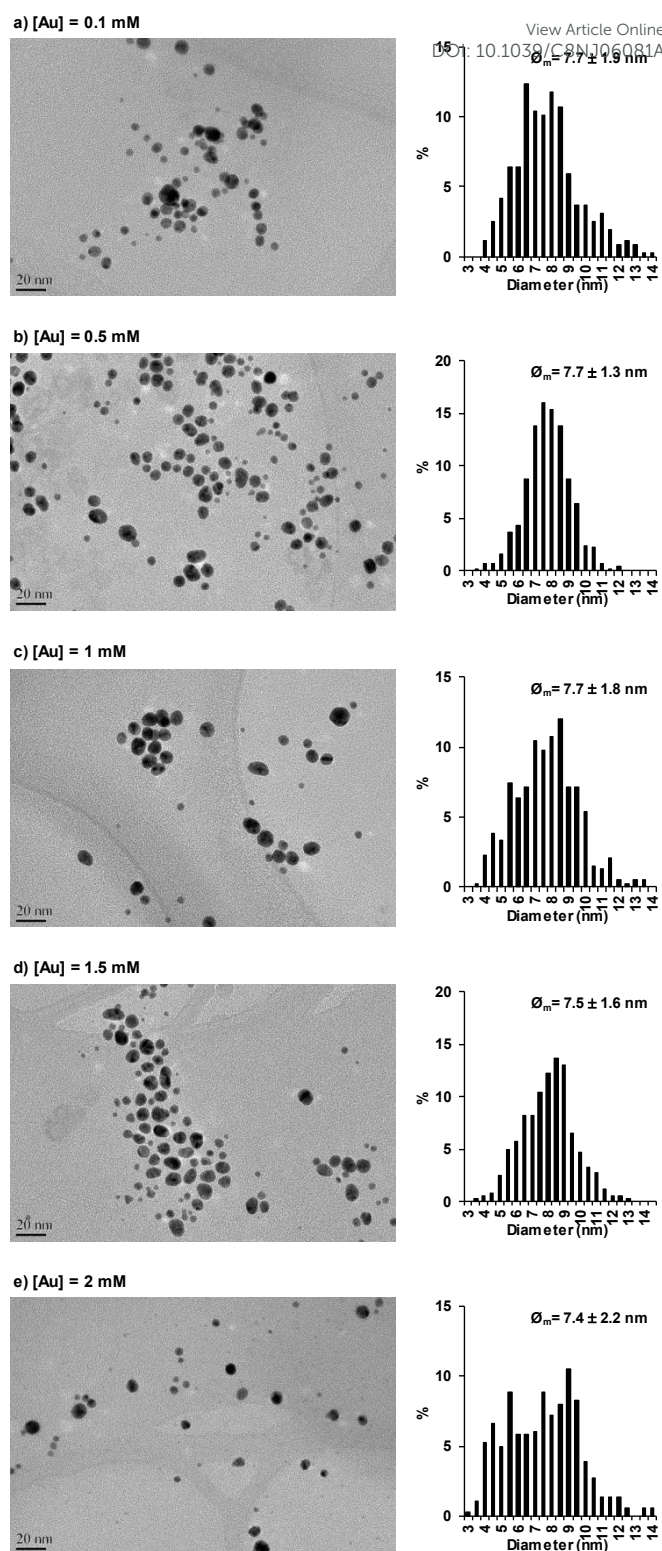
Fig. 5 TEM images and corresponding size distributions of AuNPs embedded in α-CD/Tetronics®90R4 hydrogel at (a) [Au] = 0.1 mM ; (b) [Au] = 0.5 mM ; (c) [Au] = 1 mM ; (d) [Au] = 1.5 mM and (e) [Au] = 2 mM.

ARTICLE

**Table 1** AuNP-catalyzed hydrogenation of styrene in α-CD/Tetronic®90R4 hydrogel.[a]

Entry	[AuCl$_3$] (mmol/L)	Conv. (%)[b]
1	0.1	69
2	0.5	48
3	1	45
4	1.5	35
5	2	32

[a]Conditions: styrene (50 equiv/Au), α-CD (0.75 mmol, 1250 mg), Tetronics®90R4 (0.17 mmol, 725 mg), water (5 mL), 40 bar H$_2$, 50 °C, 30 min, 1000 rpm. [b]determined by GC analysis.

It should be noticed that to have a better understanding of the catalytic process, control experiments have been carried out. First, AuCl$_3$ was solubilized in water without any additive and the resulting yellow solution was stirred under standard experimental conditions. After 1 h, the color of the solution remained unchanged. No reduction of the gold precursor was detected under hydrogen pressure. Moreover, in the case of styrene hydrogenation, no catalytic activity was obtained with AuCl$_3$ alone. Another control experiment consisted in solubilizing AuCl$_3$ int water in the presence of Tetronics®. After addition of styrene and considering the same experimental conditions described above, the color of the solution changed after 1 h of reaction from yellow to deep purple with metal sedimentation. Indeed, because of the presence of Tetronics®, it was possible to reduce the metallic precursor during the catalytic test. Nevertheless, the Au NPs sedimentation resulted in reproducibility issues and the catalytic result was not relevant. These control experiments clearly show Au NPs are the active catalyst and the addition of α-CD is mandatory to avoid any aggregation of Au NPs during the catalytic process in sol state.

Recyclability of the catalytic system

The reusability of the nanoparticle catalytic system was assessed using styrene as substrate under 40 bar of H$_2$ at 50 °C (Fig. 6).
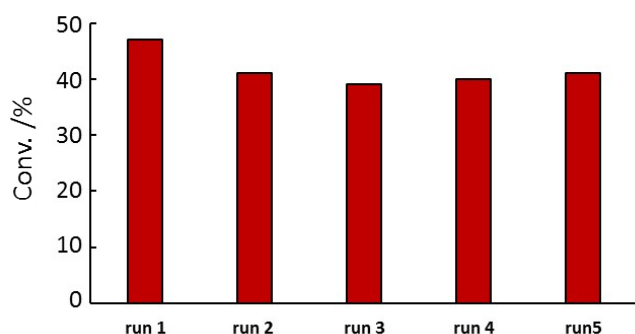

Fig. 6 Recyclability of AuNP@α-CD/Tetronics®90R4 in hydrogenation of styrene over 5 consecutive runs. [a]Conditions: styrene (0.125 mmol, 13 mg), AuNP@α-CD/Tetronics®90R4 ([Au]= 0.5 mM in 0.75 mmol α-CD + 0.17 mmol Tetronics®90R4), water (5 mL), 40 bar H$_2$, 50 °C, 40 bar of H$_2$, 30 min.

After each run, the organic phase was removed and fresh styrene was added on the hydrogel mixture. The catalytic system displayed good reusability as the conversion remained roughly the same

around 40% upon recycling. To explain the decrease in catalytic activity observed after the first run, additional experiments were carried out. The organic phase recovered from the first run was reused at 50 °C under 40 bar of H$_2$ with fresh styrene in α-CD/Tetronics®90R4 hydrogel without AuNPs (Fig. 7). As shown by the orange line in Fig. 7, the organic phase recovered after the first run was catalytically active. The increase in conversion suggested that a small proportion of AuNP was not properly immobilized within the hydrogel matrix just after the reduction of gold salts, and migrated into the organic phase during the first run (leaching). However, the remaining AuNPs in the hydrogel matrix were well stabilized, as the conversion no longer varied using the organic phase resulting from the second run. This was confirmed by TEM images of AuNPs embedded in hydrogels resulting from runs 1, 2 and 3 (Fig. 8). The distribution remained roughly constant throughout the catalytic process, thus demonstrating the robustness of the AuNP@α-CD/Tetronics®90R4 system.

Other substrates

Given the promising results obtained in the AuNP-catalyzed hydrogenation of styrene, the substrate scope of AuNP@α-
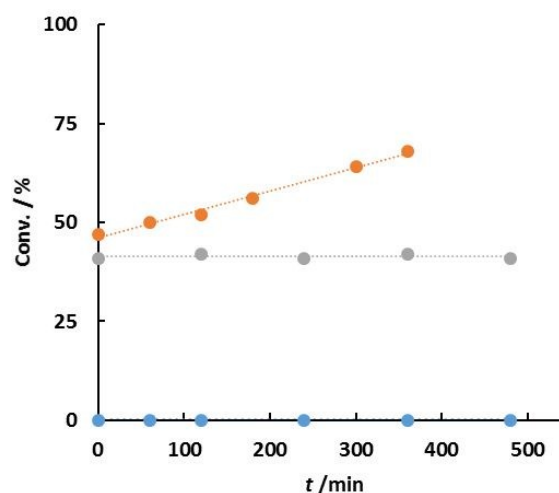

Fig. 7 Variation of the conversion over time. ● organic phase control (carried out without catalyst), ● organic phase after run 1, ● organic phase after run 2. Conditions: See **Fig. 6**.

CD/Tetronics®90R4 was evaluated using different alkenes under 40 bar of H$_2$ at 50 °C for 1h. It should be noticed that the comparison with previous reported works is not so obvious. Indeed, most of the catalytic systems reported in the literature using gold nanoparticles for hydrogenation reaction in gas phase or liquid phase are heterogeneous catalysts where influence of the support on the catalytic activity and selectivity is not negligible.[48-53]

a)

b)

c)

d)
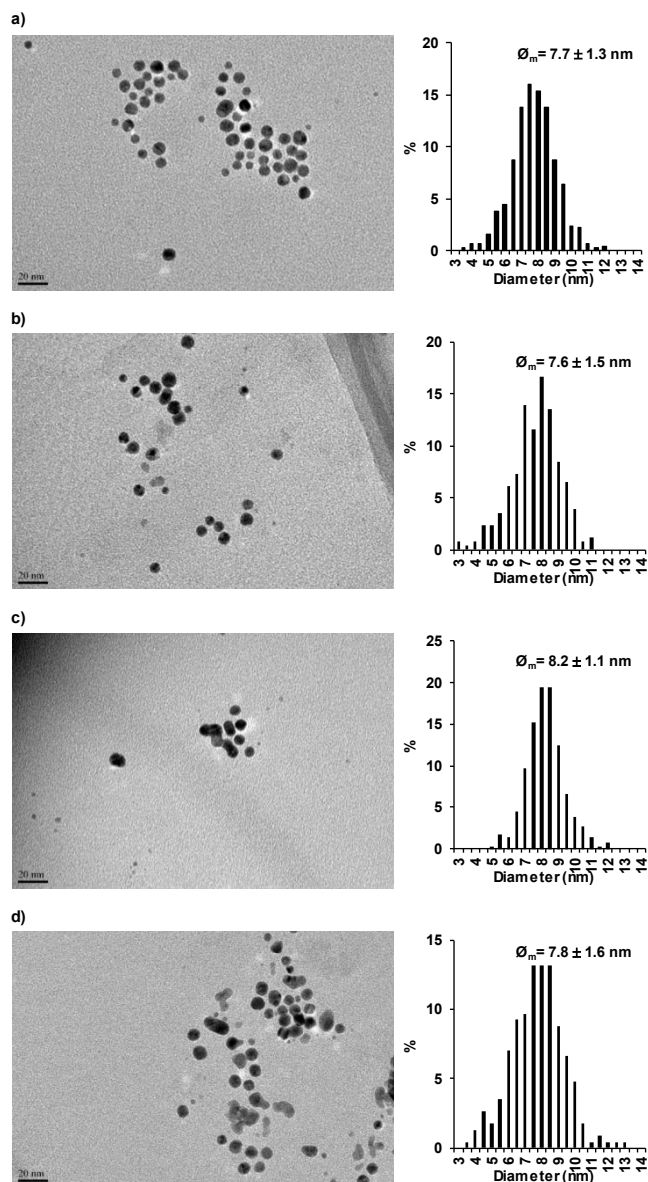
Fig. 8 TEM images and size distributions of AuNPs embedded in α-CD/Tetronics®90R4 hydrogel a) before catalysis and b) after run 1, c) after run 2 (b), and d) after run 3 for hydrogenation of styrene. Conditions: see Fig 6.

Only one publication is reporting the use of solvent dispersed gold NPs into aqueous phase containing surfactants such as SDS or CATB for the hydrogenation of anthracene.[54] The so-obtained conversions of unsaturated compounds are low and could be explained by the fact that gold is known to have i) a high energy barrier for hydrogen dissociation and ii) the least stable chemisorption state in comparison with metal such as Ni or Pt.[55] Styrene was rapidly converted (39%) to yield exclusively ethylbenzene (Table 2, entry 1). Addition of NaCl significantly affected the conversion (31%, entry 2) as already described for styrene (*vide supra*). Linear alkenes were equally converted into their corresponding alkanes, irrespective of the length of the alkyl chain (entries 3-5). *Trans*-2-octene gave similar conversion, suggesting that AuNP also reacted with its less accessible carbon-carbon double bond (entry 6). While allylbenzene gave 34% conversion (entry 7), conjugated C=C of cinnamaldehyde was not

hydrogenated at all within 1h (entry 8). Interestingly, benzaldehyde gave a low 5% conversion with excellent selectivity in benzyl alcohol,

Table 2 AuNP-catalyzed hydrogenation of terminal and internal alkenes in α-CD/Tetronic®90R4 hydrogel.[a]

Entry	Substrate	Conv. (%)[b]	Sel.[b]
1	styrene	39	100% ethylbenzene
2[c]	styrene	31[d]	100% ethylbenzene
3	1-octene	21	100% octane[e]
4	1-decene	22	100% decane[e]
5	1-dodecene	19	100% dodecane[e]
6	*trans*-2-octene	20	100% octane
7	allylbenzene	34	100% propylbenzene
8	cinnamaldehyde	0	-
9	benzaldehyde	5	100% benzyl alcohol
10	1-heptyne	8	61% 1-heptene / 39% heptane
11	1-octyne	18	53% 1-octene / 47% octane
12	1-nonyne	14	58% 1-nonene / 42% nonane
13	phenylacetylene	15	74% styrene / 26% ethylbenzene
14	citronellal	54	99% 3,7-dimethyloctanal / 1% 3,7 dimethyloctanol[f]
15	β-pinene	15	66% *cis*-pinane / 34% *trans*-pinane
16	α-pinene	9	64% *cis*-pinane / 36% *trans*-pinane
17	methyl oleate	0	-
18	methyl linoleate	0	-

[a]Conditions: alkene/Au = 100, AuNP@α-CD/Tetronics®90R4 ([Au]= 0.5 mM in 0.75 mmol α-CD + 0.17 mmol Tetronic®90R4), water (5 mL), 40 bar H$_2$, 50 °C, 1 h, 1000 rpm. [b]determined by ^{1}H NMR. [c]with NaCl (17 mg added during the synthesis of the colloidal suspension). [d]AuNPs at the interface (colorless aqueous phase). [e]no isomerization. [f]no citronellol.

indicative of the ability of the catalytic system to reduce C=O as well (entry 9). The versatility of the AuNP@α-CD/Tetronics®90R4 was also demonstrated in hydrogenation of alkynes. Mixtures of alkenes and alkanes were obtained, alkenes being logically intermediates before conversion into alkanes (entries 10-12). Phenylacetylene was selectively hydrogenated into styrene and ethylbenzene, with a

ARTICLE

styrene/ethylbenzene selectivity ratio of 74/26, without alteration of the phenyl group (entry 13). This catalytic result is in line with previous published works because gold NPs are known to be interesting in the semi-hydrogenation of alkynes into their corresponding alkenes.[56-59]

The substrate scope was further extended to biosourced substrates. The best results were obtained for citronellal (54% conversion; almost exclusively 3,7-dimethyloctanal, entry 14). This selectivity is not surprising because the isolated C=C double bond can be hydrogenated more easily than C=O double bond.[60] Hydrogenation of β-pinene and α-pinene yielded mixtures of *cis* and *trans* isomers in 2/1 proportion (entries 15 and 16). Methyl oleate and methyl linoleate showed no conversion probably because of the lower diffusion of such very hydrophobic substrates within the viscous liquid-liquid biphasic system (entries 17 and 18). Note that the activities obtained in olefins hydrogenation are lower in comparison to aromatics and alkynes. This difference could be explained by a better adsorption of aromatic compounds[61] and alkynes[50,56] onto Au(111) surface compared to alkenes.

Conclusions

With the aim of recycling nanoparticle catalysts, we developed a catalytic system consisting of AuNP embedded in α-CD/Tetronics®90R4 hydrogels. AuNP displayed an average size of ca.7 nm and a narrow distribution, as determined by TEM. The AuNP/α-CD/Tetronics®90R4 system proved to be stable over time. Upon heating above the gel-to-sol transition temperature, the studied catalytic system proved versatile, as a wide range of substrates such as alkenes, alkynes and aldehydes could be converted under biphasic conditions. The best results were obtained in AuNP-catalyzed hydrogenation of citronellal (54% conversion within 1h, 99% selectivity in 3,7-dimethyloctanal). Interestingly, upon repeated heating/cooling cycles, the AuNP@α-CD/Tetronics®90R4 catalytic system could be recycled several times without significant decline in catalytic activity.

Conflicts of interest

There are no conflicts to declare.

Acknowledgements

References

1   M. Ferreira, F. Jérôme, H. Bricout, S. Menuel, D. Landy, S. Fourmentin, S. Tilloy and E. Monflier, *Catal. Commun.,* 2015, **63**, 62.
2   F. Jérôme, M. Ferreira, H. Bricout, S. Menuel, E. Monflier and S. Tilloy, *Green Chem.*, 2014, **16**, 3876.
3   S. Noël, B. Léger, A. Ponchel, K. Philippot, A. Denicourt-Nowicki, A. Roucoux and E. Monflier, *Catal. Today*, 2014, **235**, 20.
4   G. Criny, *Chem. Rev.*, 2014, **114**, 10940.
5   L. Voorhaar and R. Hoogenboom, *Chem. Soc. Rev.*, 2016, **45**, 4013.
6   J. Potier, S. Menuel, E. Monflier and F. Hapiot, *ACS Catal.*, 2014, **4**, 2342.
7   J. Potier, S. Menuel, M.-H. Chambrier, L. Burylo, J.-F. Blach, P. Woisel, E. Monflier, and F. Hapiot, *ACS Catal.*, 2013, **3**, 1618.
8   B. Léger, S. Menuel, A. Ponchel, F. Hapiot,and E. Monflier, *Adv. Synth. Catal.*, 2012, **354**, 1269.
9   M. Almeida, M. Magalhaes, F. Veiga and A. Figueiras, *J. Polym. Res.*, 2018, **25**, 31.
10 S. Tan, K. Ladewig, Q. Fu, A. Blencowe and G.G. Qiao, *Macromol. Rapid Commun.*, 2014, **35**, 1166.
11 E. Larrañeta and J.R. Isasi, *Langmuir*, 2012, **28**, 12457.
12 M. Chevry, T. Vanbésien, S. Menuel, E. Monflier and F. Hapiot, *Catal. Sci. Technol.,* 2017, **7**, 114.
13 B. Jing, X. Chen, X. Wang, Y. Zhao and H. Qiu, *ChemPhysChem*, 2008, **9**, 249.
14 Z. Sanping, C. Mengjie, L. Liyan and W. Weilin, *Acta Chim. Sinica*, 2011, **69**, 492.
15 S. Zhao, F. Zhou and R. Liu, *Supramol. Chem.*, 2013, **25**, 767.
16 J. Yu, W. Ha, J. Sun and Y. Shi, *ACS Appl. Mater. Interfaces*, 2014, **6**, 19544.
17 L. Chen, H. Chen, X. Yao, X. Ma and H. Tian, *Chem. Asian J.*, 2015, **10**, 2352.
18 Y. Niu, X. Yuan, Y. Zhao, W. Zhang and L. Ren, *Macromol. Chem. Phys.*, 2017, **218**, 1600540.
19 H. Jia, D. Schmitz, A. Ott, A. Pich and Y. Lu, *J. Mater. Chem. A*, 2015, **3**, 6187.
20 V. Singh, P. Khullar, P.N. Dave, A. Kaura, M.S. Bakshi and G. Kaur, *Phys. Chem. Chem. Phys.*, 2014, **16**, 4728.
21 Z. Zhang and C. Shou, *J. Appl. Polym. Sci.*, 2011, **122**, 2849.
22 S.K. Ghosh and T. Pal, *Chem. Rev.*, 2007, **107**, 4797.
23 A. Villa, N. Dimitratos, C.E. Chan-Thaw, C. Hammond, G.M. Veith, D. Wang, M. Manzoli, L. Prati and G. Hutchings, *Chem. Soc. Rev.*, 2016, **45**, 4953.
24 V. Amendola, R. Pilot, M. Frasconi, O.M. Marago and M.A. Iati, *J. Phys. Condens. Matter*, 2017, **29**, 203002.
25 K. Rahme, J. Oberdisse, R. Schweins, C. Gaillard, J.-D. Marty, C. Mingotaud and F. Gauffre, *ChemPhysChem*, 2008, **9**, 2230.
26 K. Rahme, P. Vicendo, C. Ayela, C. Gaillard, B. Payré, C. Mingotaud and F. Gauffre, *Chem. Eur. J.* 2009, **15**, 11151.
27 P. Alexandridis, M. Tsianou, *Eur. Polym. J.* 2011, **47**, 569.
28 R. Ciganda, N. Li, C. Deraedt, S. Gatard, P. Zhao, L. Salmon, R. Hernandez, J. Ruiz and D. Astruc, *Chem. Commun.* 2014, **50**, 10126.
29 Y. Liu, K.B. Male, P. Bouvrette and J.H.T. Luong, *Chem. Mater.* 2003, **15**, 4172.
30 A.V. Kabashin, M. Meunier, C. Kingston and J.H.T. Luong, *J. Phys. Chem. B* 2003, **107**, 4527.
31 J.P. Sylvestre, A.V. Kabashin, E. Sacher, M. Meunier and J.T.H. Luong, *J. Am. Chem. Soc.* 2004, **126**, 7176.
32 T. Huand, F. Meng and L. Qi, *J. Phys. Chem. C,* 2009, **113**, 13636.
33 G. Stiufiuc, V. Toma, A.I. Moldovan, R. Stiufuc and C.M. Lucaciu, *Dig. J. Nanomater. Bios.* 2017, **12**, 1089.
34 M. Del Pozo, E. Blanco, P. Hernandez, J.A. Casas and C. Quintana, *J. Nanopart. Res.* 2018, **20**, 121.
35 M. Grzelczak, J. Perez-Juste, P. Mulvaney and L. M. Liz-Marzan, *Chem. Soc. Rev.*, 2008, **37**, 1783.

ARTICLE

36 M. Eguchi, D. Mitsui, H.L. Wu, R. Sato and T. Teranishi, *Langmuir*, 2012, **28**, 9021.

37 Y. Yan, P.P. Pillai, J.V.I. Timonen, F.S. Emami, A. Vahid and B.A. Grzybowski, *Langmuir*, 2014, **30**, 9886.

38 Y. Xie, D. Kocaefe, C. Chen and Y. Kocaefe, *J. Nanomater.*, 2016, Article ID 2302595.

39 N. Sahiner, *Progress Polym. Sci.*, 2013, **38**, 1329.

40 D. Zare, A. Akbarzadeh and N. Bararpour, *Int. J. Nanosci. Nanotechnol.*, 2010, **6**, 223.

41 C. Wang, L. Salmon, Q. Li, M.E. Igartua, S. Moya, R. Ciganda, J. Ruiz and D. Astruc, *Inorg. Chem.*, 2016, **55**, 6776.

42 E. Boisselier, A.K. Diallo, L. Salmon, C. Ornelas, J. Ruiz and D. Astruc, *J. Am. Chem. Soc.*, 2010, **132**, 2729.

43 K. Zabetakis, W.E. Ghann, S. Kumar and M.-C. Daniel, *Gold Bull.*, 2012, **45**, 203.

44 R. Pamies, J.G.H. Cifre, V.F. Espin, M. Collado-Gonzalez, F.G.D. Banos and J.G. Torre, *J. Nanopart. Res.*, 2014, 16, 2376–2387.

45 D. Alba-Molina, M.T. Martin-Romero, L. Camacho and J.J. Giner-Casares, *Appl. Sci.*, 2017, **7**, 916.

46 W. Gao, T.A. Baker, L. Zhou, D.S. Pinnaduwage, E. Kaxiras and C.M. Friend, *J. Am. Chem. Soc.*, 2008, **130**, 3560.

47 T.A. Baker, C.M. Friend and E. Kaxiras, *J. Am. Chem. Soc.*, 2008, **130**, 3720.

48 C. Kartusch and J.A. van Bokhoven, *Gold Bull.*, 2009, **42**, 343.

49 S.A. Nikolaev, L.N. Zanaveskin, V.V. Smirnov, V.A. Averyanov and K.L. Zanaveskin, *Russ. Chem. Rev.*, 2009, **78**, 231.

50 L. McEwan, M. Julius, S. Roberts and J.C.Q. Fletcher, *Gold Bull.*, 2010, **43**, 298.

51 T. Mitsudome and K. Kaneda, *Green Chem.*, 2013, **15**, 2636.

52 F. Cardenas-Lizana and M.A. Keane*, J. Mater. Sci.*, 2013, **48**, 543.

53 G.C. Bond, *Gold Bull.*, 2016, **49**, 53.

54 J.P. Deng, W.C. Shih and C.Y. Mou, ChemPhysChem, 2005, 6, 2021.

55 B. Hammer, J.K. Norskov, *Nature*, 1995, **376**, 238.

56 Y. Segura, N. Lopez and J. Perez-Ramirez*, J. Catal.*, 2007, **247**, 383.

57 L. Shao, X. Huang, D. Teschner and W. Zhang, *ACS Catal.*, 2014, **4**, 2369.

58 G. Vilé and J. Perez-Ramirez, *Nanoscale*, 2014, **6**, 13476.

59 T. Mitsudome, M. Yamamoto, Z. Maeno, T. Mizugaki, K. Jitsukawa and K. Kaneda, *J. Am. Chem. Soc.*, 2015, **137**, 13452.

60 P.N. Rylander, in: Catalytic Hydrogenation in Organic Synthesis, Academic Press, London, 1979, 74.

61 S.M. Wetterer, D.J. Lavrich, T. Cummings, S.L. Bernasek and G. Scoles, *J. Phys. Chem. B*, 1998, **102**, 9266.

Graphical abstract